



**HAL**  
open science

# Thermolatent Heterogeneous Epoxy–Acid Formulation for the Manufacture of Preimpregnated Sheets and Composites with Vitrimer Properties

Quentin-Arthur Poutrel, Ianis Retailleau, Ugo Lafont, Olivier Damiano, François Tournilhac

► **To cite this version:**

Quentin-Arthur Poutrel, Ianis Retailleau, Ugo Lafont, Olivier Damiano, François Tournilhac. Thermolatent Heterogeneous Epoxy–Acid Formulation for the Manufacture of Preimpregnated Sheets and Composites with Vitrimer Properties. *ACS Applied Polymer Materials*, 2023, 5 (8), pp.6095-6106. 10.1021/acsapm.3c00778 . hal-04179218

**HAL Id: hal-04179218**

**<https://hal.science/hal-04179218v1>**

Submitted on 17 Oct 2023

**HAL** is a multi-disciplinary open access archive for the deposit and dissemination of scientific research documents, whether they are published or not. The documents may come from teaching and research institutions in France or abroad, or from public or private research centers.

L'archive ouverte pluridisciplinaire **HAL**, est destinée au dépôt et à la diffusion de documents scientifiques de niveau recherche, publiés ou non, émanant des établissements d'enseignement et de recherche français ou étrangers, des laboratoires publics ou privés.

# **Thermolatent heterogeneous epoxy acid formulation for manufacture of pre-impregnated sheets and composites with vitrimer properties.**

Quentin-Arthur Poutrel<sup>a</sup>, Ianis Retailleau<sup>a</sup>, Ugo Lafont<sup>b</sup>, Olivier Damiano<sup>c</sup>, François Tournilhac<sup>a,\*</sup>

<sup>a</sup> Molecular, Macromolecular Chemistry, and Materials, ESPCI-Paris PSL, CNRS, 10 rue Vauquelin, 75005 Paris, France;

<sup>b</sup> ESTEC, European Space Agency, Keplerlaan 1, NL 2200 AG, Noordwijk, The Netherlands;

<sup>c</sup> Thales Alenia Space, 5 allée des Gabians, 06156 Cannes la Bocca, France.

## **Author information.**

Corresponding author. François Tournilhac. francois.tournilhac@espci.fr orcid.org/0000-0002-2478-0393

Author. Quentin-Arthur Poutrel. orcid.org/0000-0002-4059-2173

Author. Ianis Retailleau. <https://orcid.org/0009-0001-6558-425X>

Author. Ugo Lafont. orcid.org/0000-0002-4925-7240

Author. Olivier Damiano. orcid.org/0009-0005-9203-0059

**Keywords:** CFRP composites; carbon fibers; epoxy vitrimer; prepreg, latency.

## **ABSTRACT**

The goal of this work is to develop carbon fibers reinforced polymer (CFRP) composites showing vitrimer properties and manufacturable by the prepreg technique. Since their invention in 2011 epoxy vitrimer matrices have shown appealing potential to produce CFRP with healing, adhesion and recycling abilities. While techniques such as resin infusion or resin transfer moulding have been successfully applied, production of composites by handling of pre-impregnated sheets requires a specific set of properties which is still lacking. Starting from commercially available monomers, we hereby investigate the design and preparation of a thermolatent reactive composition compliant with the prepreg technique. The designed composition is heterogeneous, being comprised of a crystalline hardener dispersed in novolac-based epoxy resin. It thus offers i) latency and the required viscosity profile for impregnation of carbon fibers around 100°C; ii) chemical inertness and tackiness for storage and handling at room temperature, and iii) awakened reactivity for cure at higher temperature (>130°C). The whole CFRP composites manufacture (from resin mixing, impregnation and composite curing) was transferred from laboratory to an industrial environment. The resulting CFRP vitrimer composites are investigated in regard to mechanical properties, interfacial welding, damage healing and reprocessing through chemical depolymerization allowing to recover carbon fiber sheets with limited damage.

## Introduction

Modern composites, comprised of a polymer matrix and fibers (carbon, glass, polyamide, etc.) are widely used in demanding applications such as automotive, aerospace, building, sporting goods, boats, etc.<sup>1,2</sup> These composites, called fibers reinforced polymers (FRP) often incorporate an epoxy based polymer as matrix.<sup>3</sup> The assets of the epoxy chemistry are i) the wide range of commercially available resins and curing agents with virtually infinite combinations thereof, ii) a state of low viscosity before curing, permitting efficient impregnation of fibers and iii) curability without solvent, with almost no shrinkage and without by-products.<sup>4,5</sup> The existence of a liquid state before curing is of utmost practical importance as it determines the suitability of the system to be implemented by any manufacturing method. Before curing, the reactants are usually combined as to form a more or less fluid mixture, giving the possibilities to be processed in various manners such as infusion, resin transfer moulding, as well as assembly of pre-impregnated filaments or sheets. Epoxy resins are thus very well suited for manufacturing complex and high quality parts but they come with the inherent drawbacks of thermosets: repair is not possible, assembly of composite parts requires gluing or bolting, inducing weight increase in lightweight structures or even compromising the mechanical properties of those structures.<sup>2</sup> Moreover, in current time (2023), the environmental and economic impact of such thermoset structures is questioned. The chemically crosslinked nature of such polymer matrices makes them hard to recycle, giving choice of either waste landing, incineration, pyrolysis, or using harsh chemicals to attack the polymer matrix.<sup>6</sup> On top of being energetically intensive, those recycling techniques damage fibers making them only usable in the form of short strands, degrading the most expensive component of FRP composites.

In this context, vitrimers constitute an interesting alternative to regular thermosets.<sup>7</sup> Vitrimers are fully crosslinked chemical networks, yet able to exchange bonds upon thermal excitation. Unlike chemically adaptable networks where bonds are said *reversible*, being opened and closed by effect of temperature, bonds in vitrimers are said *exchangeable*, meaning the topology of the network can change but the number of links in the system is constant.<sup>7,8</sup> Vitrimers are intrinsically insoluble, like thermosets but have the ability to flow upon elevation of temperature, unlike thermosets. The link-exchange ability leads to attractive properties such as stress relaxation, controlled creep, healing, reprocessing or even chemical depolymerization in relatively innocuous solvents (*e.g.*, ethylene glycol) presently investigated through experiment<sup>9-12</sup> and simulations.<sup>13,14</sup>

The vitrimer concept was first demonstrated on epoxy networks. Notwithstanding the existence of alternative chemistry,<sup>15-22</sup> the epoxy route remains the straightforward option for transfer of the vitrimer concept in structural composite applications. Proof that epoxy vitrimers are a suitable matrix for FRP composites was made several times:<sup>12,23-26</sup> Chabert et al. produced vitrimer matrices with exchangeable ester links and a  $T_{\alpha}$  value  $> 100^{\circ}\text{C}$ .<sup>24</sup> Composites containing more than 50 vol% of continuous glass fibers showed high bonding strength and repeated welding ability while their mechanical properties were comparable to those of non-vitrimer control samples. Odriozola and coll. investigated reprocessing, repair and recycling of glass-fiber reinforced composites using an epoxy-amine matrix with exchangeable disulfide links.<sup>27</sup> In these works, composite plates were manufactured from reactive mixtures showing an initial viscosity of no more than a few Pa.s as to be implemented by resin transfer moulding. Odriozola and coll. additionally reported the assembly of multilayers by compaction of fully cured sheets. Although nicely illustrating the original properties of vitrimers, fully cured impregnated sheets have the

disadvantage of showing no tack and therefore, this process does not allow precise positioning comparable with handling of classic prepregs. Repairable and recyclable woven carbon fiber reinforced composites were also reported using malleable polyimine networks.<sup>28</sup> These materials, can show a  $T_g$  up to 135°C and are sometimes also called vitrimers. These are however networks made up of condensed small molecules (aldehydes and primary amines) as to form imine bridges. The imination reaction is not a ring opening reaction: it produces water that has to be stripped out during the condensation. Furthermore the drawback of imine (or Schiff base) compounds, well known for their uses in the past in liquid crystals, is their inherent chemical, thermal and photo-physical instability.<sup>29-31</sup>

Aforementioned epoxy vitrimers compositions were all made from a homogeneous mixture of a so-called resin (the epoxy monomer) and the other reactant, called hardener. Desirably, the hardener is well molten and homogeneously mixed as to be poured or injected within a few minutes and reacted shortly after. This makes sense when preparing bulk samples or composites through injection, infusion or resin transfer techniques where sedimentation or separation of components may lead to inhomogeneity in the cured system. In the prepregs case, the resin has to be impregnated and stored for occasionally a very long time before lay-up. Having a heterogeneous, yet homogenizable formulation may be a route to obtain tackiness and latency at ambient temperature and awakened reactivity at higher temperature. Hence, we turned our attention to recent vitrimer formulations using a high melting point crystalline hardener.<sup>32,33</sup>

Those networks proved to work with the vitrimer chemistry producing high glass transition networks, suitable to FRP composites. When attempting to transfer such formulations from laboratory to a larger scale workshop or factory, the key point is the knowledge of the operating window, including the viscosity profile, chemical conversion and exothermicity issues, as a

function of temperature and time. Here, we investigate the capacity of such heterogeneous network, comprised of a viscous epoxy-novolac resin and a crystalline dicarboxylic acid, to show i) a low viscosity ( $< 100$  Pa.s, preferably  $< 10$  Pa.s) for impregnation of high volume fractions of fibers and latency (one or a few hours) at impregnation temperature, ii) virtually no reactivity over weeks at the so-called storage temperature (preferably room temperature, or below) and iii) fast reactivity at a temperature higher than the impregnation one, giving rise to a homogeneous polymer matrix, but desirably as low as possible. Observations combining thermalized ATR-IR spectroscopy, optical microscopy and rheology are used to determine the physical and chemical state at any step of the process. Processing conditions thus developed in the laboratory were then passed to a subcontractor to realize large preimpregnated samples (at the  $m^2$  scale) on an industrial platform. After impregnation, layup and curing, the subsequent carbon FRP composites was mechanically tested and compared to classical thermoset CFRP. The panel was further tested to demonstrate original properties connected to the vitrimer nature of the polymer matrix such as healing, adhesion and reactive depolymerization.

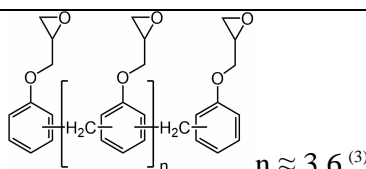
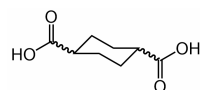
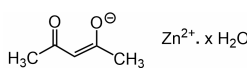
## **Experimental procedures**

### **Materials**

An epoxy-novolac resin, poly[(phenylglycidyl ether)-*co*-formaldehyde] with an average functionality of 3.6 epoxy functions per molecule, PPGEF (Epalloy 8830 from Huntsman Ltd) type was chosen for its tackiness at ambient temperature and low viscosity when heated, allowing lay-up and impregnation. Moreover, novolac resins also produce high density crosslinked networks resulting in high glass transition temperature polymers ( $> 120^\circ\text{C}$ ) usually favoured for CFRP composites. The hardener is a crystalline dicarboxylic acid (Cyclohexane-1,4-dicarboxylic

acid, CHDA from Abcr) with high melting temperature to limit potential curing at ambient temperature thus offering long latency, promotor of hydroxyl-ester links (exchangeable bonds and functions) responsible for vitrimer properties (bonding and reparability). A high melting temperature catalyst (allowing to trigger the exchange upon heating) was also chosen to limit cure at ambient temperature (zinc acetylacetonate hydrate,  $Zn(acac)_2$  from Abcr). Structure and properties of the aforementioned chemicals are given in Table 1. Octanoic acid was obtained from Alfa Aesar. All chemical were used as received without further treatment.

**Table 1:** Chemical structure and properties of the three compounds used in the preparation of latent reactive mixtures.

| Monomers            | Epoxy   | Hardener   | Catalyst  |
|---------------------|---|--|---|
| Name <sup>(1)</sup> | PPGEF   | CHDA   | $Zn(acac)_2$  |
| Formula             |  |  |  |
| Molar mass          | 171-183 g/mol <sup>(2)</sup>  | 172.18 g/mol   | 263.59 g/mol  |
| Properties          | Viscosity (52°C):<br>20 - 30 Pa.s <sup>(3)</sup>                                    | Melting T°:<br>164 - 167°C   | Melting T°:<br>135-138°C  |
| Suppliers           | Huntsman Ltd.   | Abcr   | Abcr  |

(1) PPGEF: poly[(phenylglycidyl ether)-co-formaldehyde], CHDA: Cyclohexane-1,4-dicarboxylic acid,  $Zn(acac)_2$ : Zinc (II) acetyl acetate hydrate. (2) Epoxy equivalent weight. (3) Manufacturer's specification

The chosen carbon fiber is of the plain weave unidirectional (UD PW) type with a nominal weight of 160 g/m<sup>2</sup>. As the impregnation is to be performed manually, a pure unidirectional tape is not suitable as individual tows need to be held together during manipulations. The selected material (HS03K carbon fabric G0947 D 1040 HS from Hexcel Composites) is a 1040 mm wide ribbon with 97% of HTA fiber (7.6 yarn/mm) in the warp direction, and 3% nylon wire (4 picks/cm) in the weft direction to hold all tows together. Mechanically speaking, it can be considered as a pure unidirectional tape.

### **Reactive mixtures**

Two different compositions are hereby investigated, namely without and with the Zn(acac)<sub>2</sub> catalyst, they will be further on referred as **PPGEF-CHDA** and **PPGEF-CHDA-Zn(acac)<sub>2</sub>** respectively.

For the **PPGEF-CHDA** composition, PPGEF (10g) was heated to 100°C to decrease its viscosity (well below 30 Pa.s, see Table 1) whereupon CHDA (4.86g) was added via manual mixing (using a stainless steel spatula) before leaving the mixture cool down to ambient temperature. Whenever larger quantities were manipulated, the same procedure was applied using an overhead mechanical stirrer. The slurry thus obtained, contained small solid particles dispersed in a liquid.

For the **PPGEF-CHDA-Zn(acac)<sub>2</sub>** composition, Zn(acac)<sub>2</sub> was handled as previously reported in previous work.<sup>24,34</sup> The catalyst quantity was set to 5 mol% with respect to epoxy functional groups. At room temperature, Zn(acac)<sub>2</sub> is a powder solid, sometimes agglomerated; therefore, it was grinded in an agate mortar before being mixed with the CHDA powder. Then the mixture of powders was suspended in the epoxy resin (preheated to 100°C to soften it) as previously described for the non-catalyzed composition. At this point, the reactive mixture is ready for

impregnation of fibers. The following only concerns the preparation of fiber-free specimens and is similar for both catalyzed and non-catalyzed compositions: a 30 min degassing at 100°C, followed by a pre-cure step at 130°C for 1h, whereupon the initially white mixture turned to transparent. The pre-cured resin temperature is then raised to 145°C over 1h and left to cure 8h. An 8h postcure is then applied at 180°C.

### **Infrared spectroscopy**

Attenuated total reflection infrared (ATR-IR) spectroscopy was used to monitor the variation in concentration of reactive functions and products (epoxy and carboxylic acids for the reactants, hydroxides and ester for products) throughout the curing process, and for studying the latency of reactive mixtures at ambient temperature. A Bruker Tensor 37 spectrometer equipped with a Specac Golden Gate ATR heating cell was used for the experiments. More details on the infrared analysis and spectroscopy can be found in SI and in reference.<sup>35</sup>

### **Rheological monitoring**

An Anton Paar MCR 302 rheometer equipped with 25 mm disposable plates and operating at a constant 1 rad/s oscillatory shear was used to measure the viscosity of the epoxy resin at different temperatures and the evolution of the viscosity of the reactive mixture during cure and detect the occurrence of the gel point.

### **Thermal analysis**

Differential scanning calorimetry (DSC) measurements were performed using a DSC Q1000 analyser from TA instruments, the enthalpy signal of the investigated reactive mixtures have been

analysed according to the Kissinger di Benetto method.<sup>36,37</sup> More details on this method can be found in SI. Thermogravimetric analysis (TGA) was performed using a Netzsch Libra TG 209 F1 analyzer. The weight loss of the samples was measured from 25 °C to 600 °C at a constant rate of 10 °C/min under a nitrogen atmosphere. Dynamic mechanical analysis (DMA) was performed using a MCR 702 Anton Paar rheometer operating in the torsion mode at 1 rad.s<sup>-1</sup>, using 3°C/min ramps and 1% strain. Additional experiments using the three point bending accessory are described in SI.

### **Optical microscopy**

Polarized optical microscopy observations were made on a Leica DMRD microscope equipped with a Fluotar 5×0.12 objective, Sony XCD-100CR digital camera and Mettler FP50 heating stage. Mixtures of CHDA and PPGEF were placed between a glass slide and cover slip for temperature investigations between 80°C and 200°C.

### **Composites preparation**

Carbon fibers impregnation of m<sup>2</sup> large panels was made manually in the premises of the Kalliste Composite company (Nice France). The methodology developed in the laboratory to evaluate fiber impregnation and CFRP composites was passed on to the company as follow: for initial fibers soaking, an impregnation on both sides was considered to be optimal to maximize fibers wetting. According to viscosity measurements and curing characterization, all chemicals were mixed together at 100°C, the mixture was then applied directly on either side of the carbon fiber tissue. The mixture was kept between 100°C and 120°C and spread over with the help of a smoothing iron. The impregnated carbon fiber sheet thereby obtained was then cooled down to

room temperature and cut into smaller squares of ~30cm, these squares were laid up according to the following stacking sequence  $0^\circ / 60^\circ / -60^\circ / 0^\circ / 90^\circ / -30^\circ$ . Once stacked, the multilayer assembly was squeezed in a vacuum bag and put under pressure in an oven with the help of iron weights. The curing conditions remained similar to those of non-reinforced polymer samples:  $130^\circ\text{C}$  for 1h, a  $15^\circ\text{C/h}$  ramp until  $145^\circ\text{C}$ , an isothermal cure at  $145^\circ\text{C}$  for 8h. Finally, the composite plate was postcured 8h at  $180^\circ\text{C}$ . The resulting panel was cut into  $10\text{ cm} \times 2\text{ cm}$  samples for further testing. The fiber content was evaluated on the basis of density values (detailed calculations in SI).

Compressive tests have been performed according to ASTM D3410 standard at Thalès Alenia Space facilities. Composite samples healing was performed in the hot press at  $180^\circ\text{C}$  for 1h at 0.5 bar pressure. This procedure also led to flatten the whole samples to equivalent thicknesses and prepare them for adhesion. Composite samples welding was achieved after sanding and cleaning  $2.5\text{ cm}^2$  surfaces of CFRP. Then those surfaces were pressed against each other by pairs, as to form three lap-shear joints with an overlap area of  $2.5\text{ cm}^2$ . The lap shear specimens were placed for 1h30 at  $180^\circ\text{C}$  in a clamp comprising two M5 screws tightened with a torque of 1.7 N.m, thus ensuring a force of approximately 4000 N over the total area of  $7.5\text{ cm}^2$ . The adhesion strength was measured with an Instron 5900 machine with pneumatic clamps (pressure, 2 bars) at a deformation rate of  $1\text{ mm}\cdot\text{min}^{-1}$

## **Results & discussion**

The workflow of experiments hereby reported is presented in Figure 1. First, reactive mixtures are devised with suitable latency and viscosity profiles as to be spread on a dense layer of carbon fibers and stored for long time in the form of pre-impregnated sheets. Then, individual layers are

stacked, compressed and cured, as to form composite samples with a  $\approx 40\%$  volume fraction of crossed fiber reinforcement. Then a few properties of the composite parts are evaluated in different conditions including some new properties brought by the vitrimer nature of the matrix, such as composite healing, welding and matrix depolymerization.

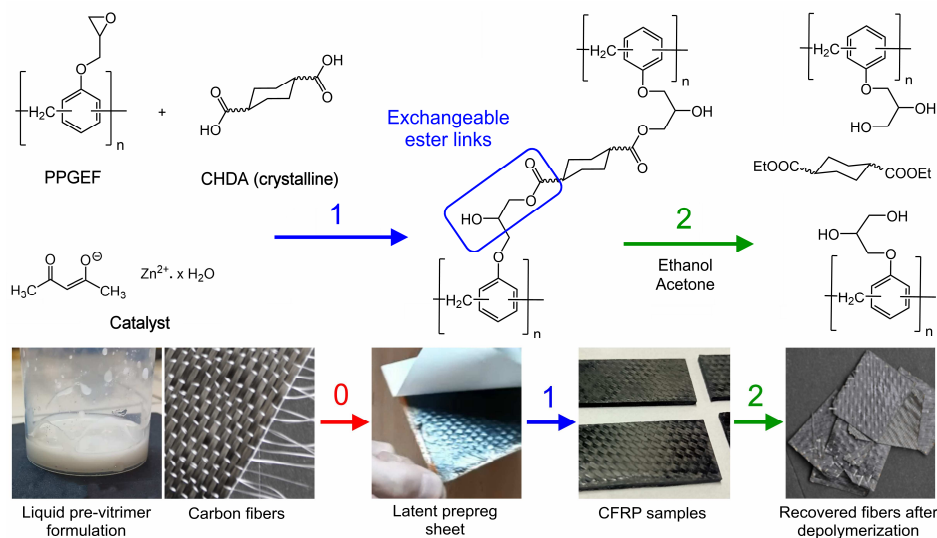


**Figure 1:** Thermolatent epoxy formulation with vitrimer-like properties: workflow from heterogeneous preparation to chemical depolymerization and fibers recovery; 0) pre-impregnation in the quiescent state, 1) epoxy-acid addition at the curing temperature, 2) chemical exchange by transesterification with the solvent.

### Formulation of a latent pre-vitrimer composition

Strategies to impart latency in epoxy formulations have been reviewed.<sup>5</sup> The most straightforward approach is to rely on the regular Arrhenius law and select an epoxy-based system showing a high activation energy, *e.g.* 100 kJ/mol or more. Such systems have been designed based on supramolecular chemistry.<sup>38,39</sup> High activation energy, in this case, means that the contrast between reaction rate at high temperature and reaction rate at low temperature is

more pronounced. The main downside of this path is that, residual reactivity at the ambient is small but finite and this affects the viscosity of the reactive mixture over time. Other strategies use macro or microphase separation, or encapsulation. There, the idea is to prevent reaction by physically separating the reactants. Dicyandiamide (DICY) which is typically used for this purpose is crystalline. This crosslinker slowly dissolves in the epoxy resin and starts to react on heating but shows no reaction at all at room temperature. Furthermore, with this reagent, crosslinking takes place through a rather complex mechanism involving both step and chain polymerization mechanisms, eventually beneficial for latency. Curing with DICY, allows to reach a Tg of about 140°C.<sup>12</sup> However, in the current state of knowledge, DICY cannot be used to produce a network with exchangeable links (Figure S1a). On the other hand, cyclic anhydrides are used for this purpose because their reaction with epoxides produces exchangeable ester links. The problem of this type of curing is that the produced networks lack of hydroxide groups, which are also necessary to activate the transesterification exchange reaction. To solve this problem, it was recently proposed to blend the reactive mixture with a rigid diglycol co-monomer to serves as a hydroxide source.<sup>40</sup> This strategy enabled to produce high-Tg epoxy-anhydride vitrimer networks with accelerated relaxation potentially suitable for CFRP composites. Yet, anhydrides show relatively low melting points and a moderate activation energy making them poorly suitable towards formulation of thermolatent compositions. Retaining the idea of a monomer or comonomer both rigid and protic but also crystalline, our choice fell here on the 1,4-cyclohexane dicarboxylic acid.<sup>32,33</sup> As for the chosen resin, it is a prepolymer of the novolac epoxy ether type, conventionally used in preregs because it has both the appropriate viscosity and a high density of crosslinkable groups. The expected curing reaction is shown in Figure 1.

Figure 2A shows the IR measurements of the reactive mixture at 25°C over a period of 25 days. There is no noticeable change in the IR spectrum of the PPGEF/CHDA mix, the characteristic signal of the epoxide (Figure 2A right panel) does not evolve over a period of 25 days indicating latency on this time scale. As for C=O stretching vibrations, neither the starting material (acids) nor the expected product (ester) is detectable (Figure 2A right panel). To explain this, it must be reminded that in the ATR technique utilized here the region scanned by the infrared radiation is not deeper than the depth of the evanescent wave,  $D_p$ , as given by equation 1.

$$D_p = \frac{\lambda}{2\pi n_1 \sqrt{\sin^2 \theta - \left(\frac{n_1}{n_2}\right)^2}} \quad (1)$$

Where  $\lambda$  is the IR wavelength,  $n_1$  and  $n_2$  the indexes of refraction of the ATR crystal and sample and  $\theta$  the incidence angle. Practically,  $D_p$  is of the order of a few microns, or less. In case of a two-phase sample, the heterogeneous distribution of the constituents in the vicinity of the interface may cause one of them to disappear. This is what is happening here, due to the granular shape of CHDA crystals, there is poor contact of this component along the interface. Thus, CHDA molecules, blocked in the crystals did not intercept the evanescent wave (to produce an ATR-IR signal the substance must form a liquid film of 0.5 - 4  $\mu\text{m}$  thickness) and did not react with the epoxy either. Hence, as long as the substance is in its crystals form, it is not detectable using ATR-IR spectroscopy, nor reactive which explains why nothing is visible in the C=O stretching region. This is further confirmed by the stability of the signal in the 2500  $\text{cm}^{-1}$ –4000  $\text{cm}^{-1}$  region (Figure 2A left panel) corresponding to the stretching of alkyl and hydroxyl functions. The mix PPGEF/CHDA without thermal treatment therefore shows chemical stability for at least 25 days at room temperature.

Latency thus proven has significance for storage, the next step is to monitor how the reactivity of the mixture at temperatures suitable for impregnation of carbon fibers. As the novolac-based epoxy resin has a drop in viscosity above 60°C (cf Table 1), we study the reactivity at three different temperatures: 100, 110, and 130°C. To assess the impregnation parameters in this processing window, we recorded the evolution of chemical species over 24h using thermally-controlled ATR-IR spectroscopy. In parallel, rheology was performed to record viscosity evolution and time to gel point. The gel point is estimated by the crossover of the storage modulus  $G'$  and loss modulus  $G''$  at 1Hz (For the curing of epoxy resins, this determination was found close to the frequency-independent value in ref.<sup>41</sup>)

Figures 2B-2D show the IR spectra of the PPGEF/CHDA mix at  $t = 0$  h and  $t = 24$ h for each temperature. The first remarkable feature is the clear appearance of the C=O signals (*oxo* and *oxy* H-bonded acids, Figure S2) due to the melting of CHDA crystals and dissolution of this reactant inside the epoxy at temperatures  $\geq 100^\circ\text{C}$ .<sup>35</sup>

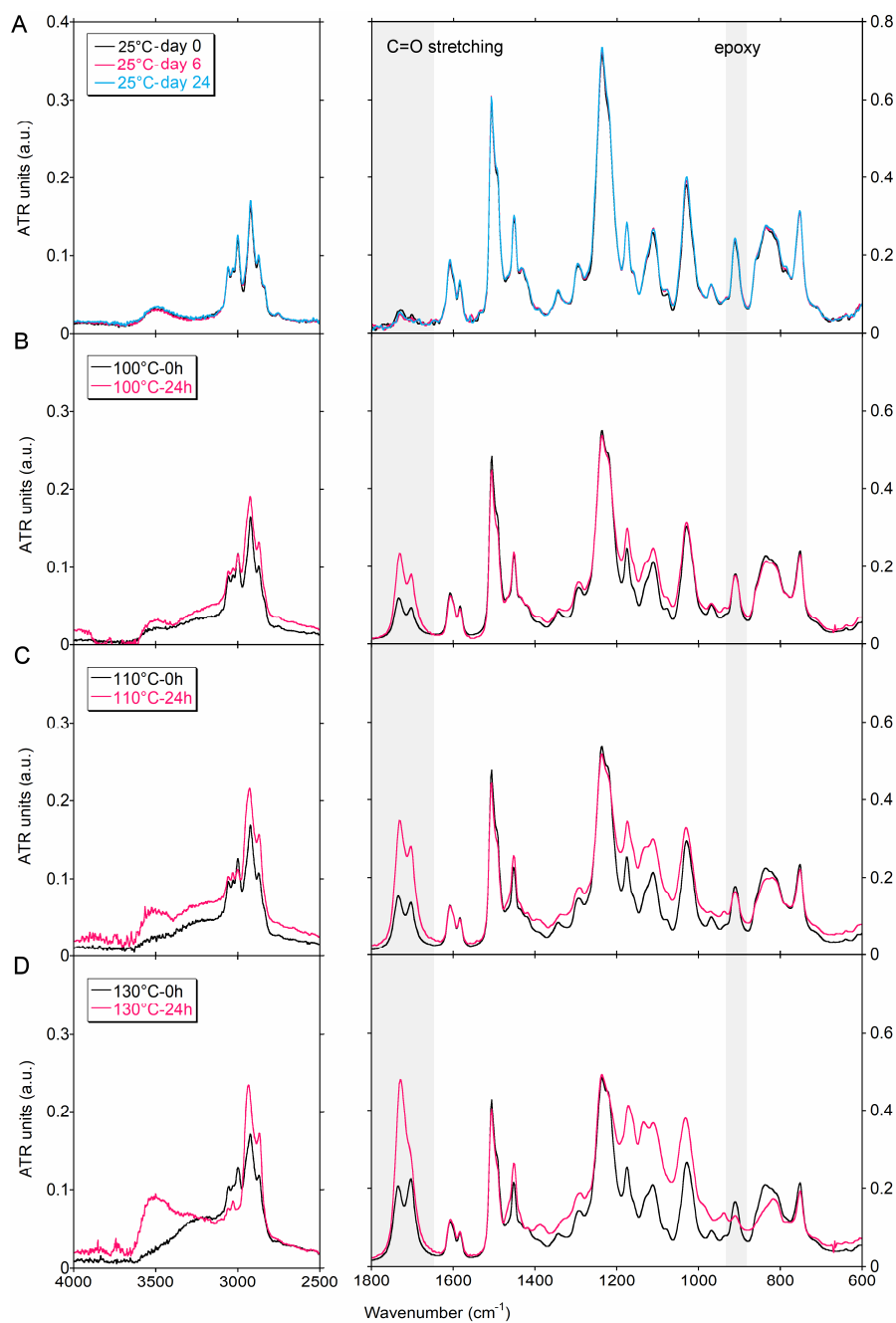


**Figure 2:** Infrared spectra of the PPGEF/CHDA mix at (A) 25°C; over a span of 25 days, no noticeable change is detected; absence of bands in the 1700  $\text{cm}^{-1}$  region demonstrate insolubility of CHDA at this temperature. B-D: comparison of IR spectra of the PPGEF/CHDA mix at  $t = 0\text{h}$  and  $t = 24\text{h}$  at: (B) 100°C, (C) 110°C, and (D) 130°C.

Furthermore, comparing the IR traces taken at  $t = 0$ h for 100°C, 110°C, and 130°C, where evidently the peaks around 1700  $\text{cm}^{-1}$  are growing, lead to the conclusion that dissolution takes place in this temperature window. After 24h at 100°C (Figure 2B) the characteristic signals of acid, epoxy and the OH stretching region (left panel) barely evolved indicating that the mixture has little reactivity and thus leaves enough time to perform impregnation. After 24h at 110°C, both epoxy and acid signals have evolved and the characteristic ester's vibration appears (Figure 2C right panel), with a clear increase of the OH stretching at 3500  $\text{cm}^{-1}$  (Figure 2C left panel), indicating that the polymerization is started but not completed (as revealed by the remaining epoxy signal after 24h (right panel)). At 130°C (Figure 2D), the characteristic signals of carboxylic acid and epoxy completely disappear within 24 h and a clear ester vibration is seen, together with the OH stretching band at 3500  $\text{cm}^{-1}$  thus indicating that the polymerization reaction is completed.

Further analysis of these monitoring was performed by integrating the signals defined earlier (*cf. experimental procedures*) over this 24h period. Figure 3 shows the evolution of the characteristic species: epoxy (a), esters (b), and the hydroxyl signal (c) of the  $\beta$ -hydroxy ester fragment. It is clear that at 100°C, the system barely reacts over 24h, upon increasing to 110°C it comes evident that the system reacts faster but is still continuously evolving after 24h. However, at 130°C, the system reacts fast for ~500-600 min (*i.e.*, > 10h), then the conversion slows down for the rest of the measurement. This indicates that most chemical moieties reacted through polymerization and once most of reactants are consumed (~80%),<sup>42</sup> the reaction slows down. Another classical reason for slackening is the vicinity of the  $T_{\text{cure}}$  and  $T_{\infty}$  ( $T_{\text{g}}$  of fully cured network) once the monomers are exhausted.

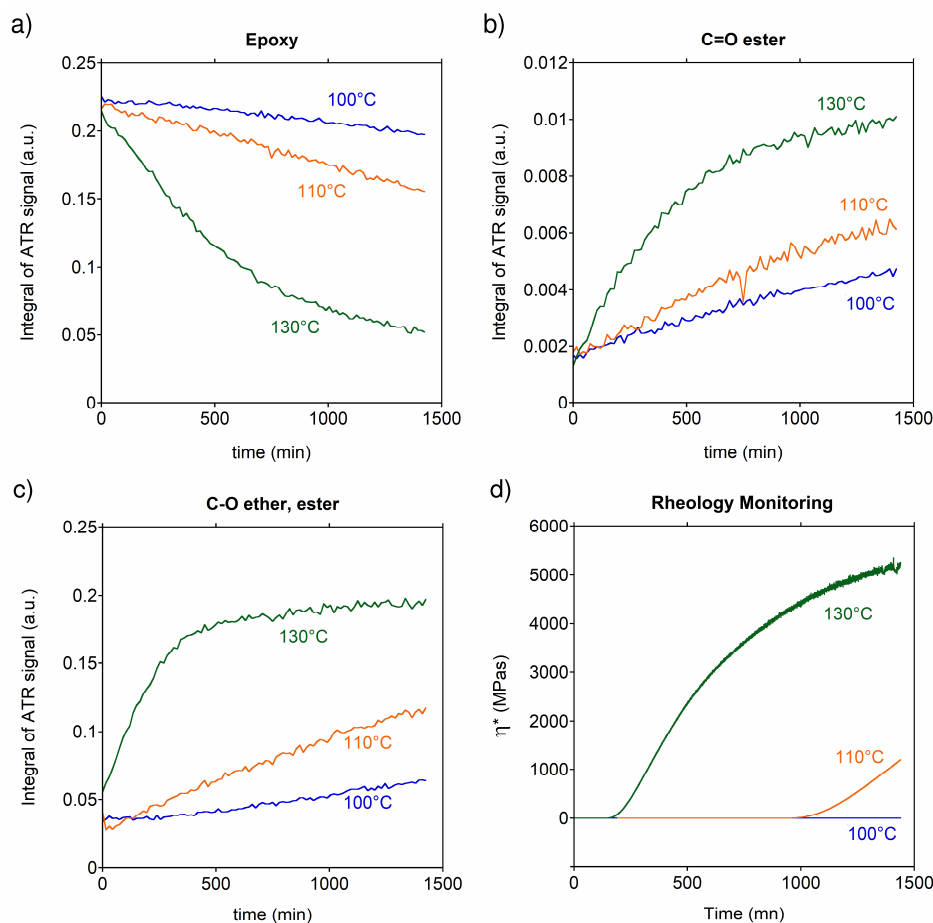


**Figure 3:** Time dependence of characteristic IR signals and complex viscosity of the PPGEF/CHDA mix over 24h at 100°C, 110°C and 130°C for: a) epoxy, b) C=O stretching vibration of ester, c) O–H stretching vibration of ester, d) complex viscosity at 1 rad/s.

Figure 3D shows the rheology measurements made on the same mixture (PPGEF/CHDA), displaying the complex viscosity over time at these temperatures. At 100°C, the system has little to no reactivity, hence, the measurement does not give particular information except that the gel point is not reached in 24h. This confirms what was observed in ATR-IR - that no esters are produced by the PPGEF/CHDA reaction. At 110°C, conversion of epoxides and carboxylic acids

happens leading to effective cross-linking. Following definition given above, the gel time at 110°C is of about 12 – 13h (crossover of G' and G'' in Fig S3). At 130°C, the gel time is reduced to about 3h. Before gelation, the viscosity of the reactive system is of 18–40 Pa.s at 110°C and 2–6 Pa.s at 130°C. At 110°C, the viscosity is in the required range with little to no reactivity for nearly 10h. The impregnation temperature was set at 100–110°C, which leaves enough time to manually impregnate large carbon fibers as shown later in this work.

The crystallinity of CHDA with high melting temperature gives, therefore, a satisfactory latency for storing, handling and impregnation of this resin type. Control experiments with octanoic acid and sebacic acid confirm this relationship: Sebacic acid is a solid (MP = 135°C), its mixture with epoxy shows no sign of reaction over 2 hours at 90°C while the ester typically forms in less than 20 min at 125°C.<sup>35</sup> Octanoic acid is a liquid. At 25°C, its mixture with PPGEF shows the carbonyl vibration in ATR. Effective dissolution at 25°C induces a drop in viscosity, detrimental to prepregs' manipulation (Figure S4); and the epoxy-acid system is known to be reactive at 100°C once dissolved.<sup>43</sup>

However, heterogeneous formulations bring challenges to obtain homogenous samples: a fast curing at high temperature led to samples with bubbles and high quantity of unreacted CHDA crystals. Meanwhile, with a temperature too low, the slow curing unfavourably allows time for sedimentation of CHDA at the bottom of the samples. Few systems already reported examples of heterogeneous networks to prepare vitrimers from crystalline hardener, including a degassing phase at elevated temperature.<sup>32,35</sup>

Per se, the application of temperature during the degassing step has not for sole purpose to decrease the resin viscosity and allow bubbles removal. In those reports, the heterogeneous mixture was reported to pass from a white color to transparent state indicating dissolution of

crystals in the resin.<sup>32,35</sup> Hence, we used optical microscopy to observe the crystals behavior within the epoxy when temperature is increased. Inspection of the raw mix in polarized optical microscopy (Figure S5) demonstrates that the CHDA crystals initially seen at room temperature are still present until 130°C, whereupon they gradually melt. At 170°C most of the crystalline phase is molten and dissolved in the optically isotropic mixture. Yet, a minority of birefringent areas are still detected, and this even at 200°C (Figure S6). This revealed that the mixture of cis/trans CHDA was comprised of crystals with inhomogeneous melting temperature. The majority of them show a melting temperature of ~170°C and are easily dissolved in PPGEF. Yet, a minority of crystals show a higher melting temperature (>200°C) and proved difficult to react. Nonetheless, from the unreacted crystals size and remaining quantity, it was concluded that the CHDA was still suitable as hardener for the formulation of vitrimer resin aiming to impregnate carbon fibers.

Rather than combining degassing and dissolution steps as in previous reports, degassing was performed at 100°C, where crystals remained in their solid form, thus keeping the latency of the system when temperature is brought back to ambient. The homogenization of the system was then performed following IR and rheology results from our data previously shown (Figure 3). We set the reactive mixture for 1h at 130°C to allow melting of most crystals while remaining far below the gel time. This "pre-curing" step led the system to pass from a white opaque aspect to transparent (Figure S7) – indicating that most CHDA crystals were dissolved in the epoxy. The remaining opacity of the resin can be attributed to the unsolvable crystal fraction observed through microscopy (Figure S5 and S6).

The infrared spectrum of the reactive mixture before heating and after 1h and 24 h curing at 130°C are presented in Figure S8. As already observed, the signal of the carboxylic acid hardener

is not detected at room temperature. At 130°C, the carboxylic acid signal (doublet at 1712 and 1740  $\text{cm}^{-1}$ ) is detected: dissolved molecules can access the interface and give rise to detectable IR absorption signals. As for the epoxy signal, its position changes between room temperature and 130°C, then, it decreases but remains present after 24 h of curing, showing slow reaction at this temperature. This is all truer since the decrease in the epoxy signal is partially due to increased volume fraction of dissolved CHDA crystals.

Right after this precuring step, characteristic signals of the carboxylic acid are then evident. As already mentioned, the C=O stretching vibration is split due to different forms of H-bonding. After long stage at 130°C, the C=O stretching vibration of the ester, has appeared at  $\sim 1725 \text{ cm}^{-1}$  but the carboxylic acid is still detected, showing effective dissolution of CHDA with slow reaction at this temperature.

Once resin homogenization was probed, a curing cycle had to be defined to achieve most epoxide/acids conversion within a reasonable amount of time. The evolution of precured samples has been monitored by ATR-IR, for different curing temperatures (100, 110, 130, 145°C). The results are shown in Figure S8 a–c, similarities between raw mix and precured resin (homogenized) in the temperature 100–130°C range demonstrate that the precuring step has for main goal to components through formation of epoxy-CHDA adducts at early stage of the reaction (see Figure S2 for detailed explanation). Nonetheless, to obtain rapid and full curing of the epoxy resin, an increase to 145°C after precured for 8h is necessary. A postcuring step at 180°C for 8h was then applied to ensure maximum conversion of remaining monomers. To go a step further in the suitability of such heterogeneous networks for CF impregnation, the intensities of two characteristic vibrations related to the COOH group are plotted (Figure S9) as a function of cure time at different temperatures. Before experiment, all samples have been subjected to a 1h

precure at 130°C. Even though O-H stretching signal has a higher level of noise, the information brought by both measurements are the same. At the initial time, the concentration of COOH increases almost linearly with temperature. Then the level remains constant at 100°C, slowly decreases at 110°C, faster at 130°C, even faster at 145°C. Interestingly, complete consumption is observed at 130 and 145°C after 24 hours but final level is almost the same as the initial one when cure is performed at 110 or 130°C.

To better visualise the behavior of the reactive mixture in temperature and understand the design of the material, Figure 4 plots the viscosity of the resin (measured by rheology), the epoxy opening reaction rates measured by the initial slope of the epoxy conversion graph (Figure 3a), and the percentage of black pixels of the images of Figures S5 and S6 (pixels with luminance under 30 in a 0–255 scale are considered black) correlated to the disappearance of CHDA crystals. On this graph appear three temperature ranges suited for the successive steps of the composite manufacturing: at low temperature (below 100°C), the reaction rate close to 0 and the high viscosity of the resin allows long latency and high tackiness for proper handling, storage and layup of prepregs sheets. At intermediate temperature (between 100 and 120°C), the reaction rate stays finite but the viscosity of the resin is low (around 200 mPa.s<sup>-1</sup>), allowing impregnation of carbon fiber sheets without reaching the gel point during the process. At high temperature (above 120°C), the reaction rate steeply increases whereas the melting of CHDA crystals is ascertained by POM. In Figure 4, the reaction rate data are fitted by a solid line corresponding to an Arrhenius activation energy of 159 kJ/mol. Such a value higher than 100 kJ/mol clearly corresponds to the above definition of a thermolatent system.

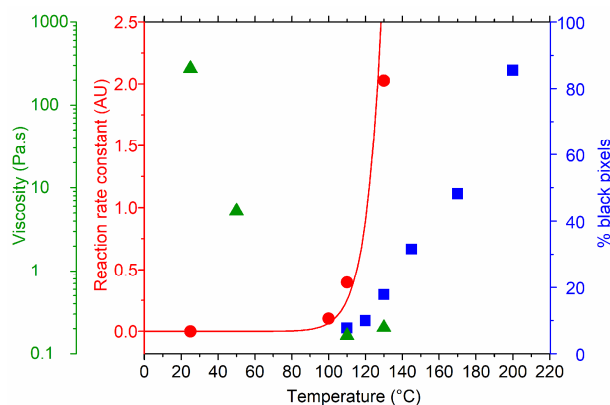


**Figure 4:** Diagram showing the correlation between epoxy resin viscosity ( $\blacktriangle$ ), effective melting of CHDA crystals ( $\blacksquare$ ) and initial reaction rate of the epoxy-acid reaction ( $\bullet$ ).

These data demonstrate that two different factors contribute to the latency of the CHDA–epoxy system: low solubility, due to its high melting point and low reactivity between 100°C and 130°C. In this temperature range, approaching but still below the melting point of CHDA (164 – 167°C), the instantaneous concentration of carboxylic acid is thus determined both by the kinetics of dissolution and that of reaction with the epoxide. Practically, this means that this composition has an excellent latency profile for impregnation of fibers but on condition that it remains in this temperature range. Otherwise, there is a risk that the system will viscosify in the event of cooling, with formation of clots as well as in the event of heating with premature hardening of the resin.

### **Resin with catalyst: PPGEF/CHDA/Zn(acac)<sub>2</sub>**

To produce a system with vitrimer properties, a catalyst for transesterification is required to display the capacity of the polymer to be weld and healed in a suitable time/temperature window. Adding a catalyst to the mixture potentially leads to several changes in the resin behavior, especially latency and curing. Hence the exact same procedure was applied to the reactive

mixture with catalyst to measure its latency over 25 days. Figure 5 shows the IR measurements of the raw mix at 25°C over this period of time. There are no noticeable changes in the IR signatures of the reactive mixture incorporating PPGEF, CHDA and Zn(acac)<sub>2</sub>, indicating that after 25 days the network has no reactivity at room temperature. This confirms latency over period of weeks for both uncatalyzed and catalyzed systems. As for stability over a longer timescale, samples of the catalyzed formulation have been stored at -18°C and re-analyzed two years later after thawing. The sample showed unchanged pasty texture at 25°C, IR analysis revealed slight solubilization of the acid and remnant epoxy groups while kinetics at 130°C demonstrates the system is still reactive (Figure S10).

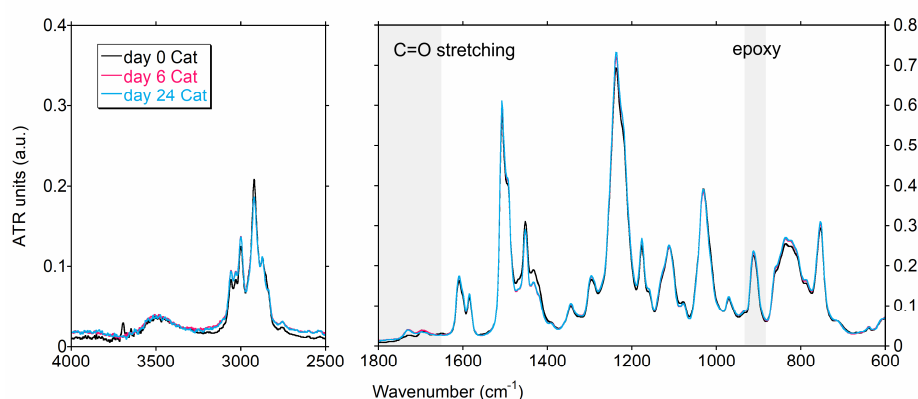


**Figure 5:** Infrared spectra of PPGEF/CHDA/Zn(acac)<sub>2</sub> mixed manually at 100°C and left to cool down to room temperature. Measurements are performed at 25°C.

To preserve latency while fostering vitrimer properties, the catalyst should not accelerate ring opening reactions. Exchange reactions are athermal and ring-opening ones are exothermic. These latter are therefore selectively monitored by DSC. The results for catalyzed and uncatalyzed systems are presented in SI (Figure S13, Tables S1, S2). In isothermal curing at 145°C, the

reaction rate is roughly the same for both systems. At higher temperatures, DSC data at variable heating rates (Kissinger method, ref<sup>44</sup>) give a measure of the activation energy,  $E_a$ . The catalysed system shows  $E_a = 65 \text{ kJ.mol}^{-1}$  while the uncatalyzed system gives  $E_a = 74 \text{ kJ.mol}^{-1}$ . These values are by far lower than the one ( $159 \text{ kJ.mol}^{-1}$ ) determined by fitting the data of Figure 4. In the Kissinger's method, the key for determination of the activation energy is the position of the reaction exotherm as a function of the heating rate. In the data presented in Table S1, the maximum exotherm always falls between 200 and 250°C. The activation energies thus determined are therefore relevant to that temperature range where the homogeneity of the reaction mixture is at its best and moreover the  $E_a$  value is not much lowered with the catalyst. This indicates that the heterogeneity of the mixture is by far the principal factor of thermolateness, and demonstrate the interest of this design.

### **Polymer characterization**

The glass transition temperature after cure was determined by dynamic mechanical analysis using a dual motor MCR702 rheometer. The uncatalyzed sample exhibits an  $\alpha$  relaxation temperature of  $T_\alpha \approx 100^\circ\text{C}$  at  $1 \text{ rad.s}^{-1}$  while the catalyzed sample has  $T_\alpha \approx 107^\circ\text{C}$  (Figure 6A and 6B respectively). The measured  $T_\alpha$  meet the objective of a vitrimer matrix with  $T_g > 100^\circ\text{C}$  for CFRP composites. Moreover, two distinct features appear from this characterization: (i) In the vicinity of  $T_\alpha$  and above, the storage and loss modulus of the catalyzed system are both higher than that of uncatalyzed one, probably due to a higher conversion at the end of the cure stage. (ii) In presence of the catalyst, the  $\tan \delta$  peak deforms with shift of the maximum towards higher temperatures. This trend, (also observed in other metal-catalyzed systems)<sup>32,35</sup> reflects a network densification,

probably due to larger involvement of alcohol + epoxy additions,<sup>22</sup> conducive to additional ether links.

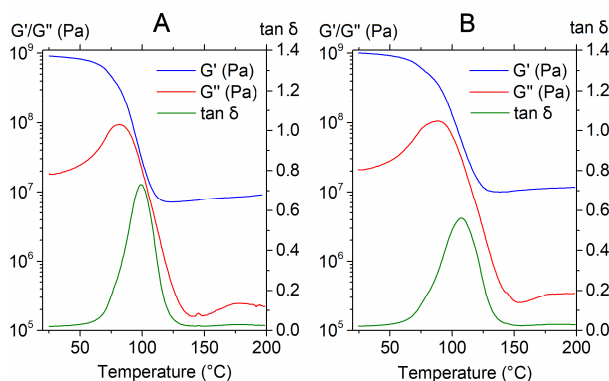


**Figure 6:** Dynamic mechanical measurement of the PPGEF CHDA system. A: without catalyst, B: with 5 mol% Zn(acac)<sub>2</sub>.

The thermal stability of the cured networks was evaluated using thermogravimetric analysis TGA under a nitrogen flow. Results are presented in Figure S15, both networks exhibit an initial weight loss in the vicinity of 100°C, probably due to the release of humidity. Then, the samples show a high temperature of degradation (> 300°C) which is classical for thermoset epoxy polymers. For the catalyzed system, the temperature of 5% weight loss is of about 325°C compared to 360°C for the uncatalyzed system. However, it can be seen that moisture evaporation is more important for the catalyzed sample. If the 5% weight loss is considered with respect to the weight at 100°C, the value is ~365°C for both samples.

## CFRP composites

The preparation of large size preimpregnated sheets is illustrated in Figure S16: After fibers impregnation, layup and curing, the resulting panel was then cut in small samples of  $10 \times 2$  cm with the help of a dry diamond saw, to proceed of CFRP characterization.

The outgassing properties of the neat matrix and its CFRP composites have been measured based upon the micro-VCM test (ECSS-Q-70-02). Data are given in Table S3, the CFRP composite presents a CVMC (Collected Volatile Condensable Material) of 0.17 % and a recovered mass loss (RML) of 0.98 %. The European Space agency recommends values of CVMC  $< 0.1\%$  and RML  $< 1\%$  for aerospace applications. This CFRP composite already satisfy the requirement of RML, and improvement of the formulation or manufacture are envisioned to reach the CVMC requirement making those long latency of vitrimer formulation suitable for use in the aerospace industry.

Compression tests were also performed and compared to the expected value of a reference thermoset CFRP composite cured with DICY. Those tests, made at different temperature ( $-70^{\circ}\text{C}$ ,  $25^{\circ}\text{C}$ ,  $60^{\circ}\text{C}/90^{\circ}\text{C}$ ) allow to strongly engage the resin and are thus a relevant test for assessing the health and quality of composite laminates, the results are collected in Table 2. For Young's modulus, the measured values bracket the expected one. As for the compressive strength, three samples were tested giving an average of about  $180 \pm 72$  MPa at ambient temperature. This result is at least 40% lower than expected, considering the strength at low temperatures (see Table 2,  $-70^{\circ}\text{C}$  value), matching the prediction, this low strength at room temperature is likely linked to early softening of the matrix, visible on the DMA plot (Figure 6). Another cause, reflected on the large dispersion of results may be the non-optimal pressure cycle (*i.e.*, with weight rather than in

autoclave) during curing. This may have an impact on its compressive strength, combining with the heat sensitivity point indicated just before.

Table 2: Calculated and measured Young's modulus and compressive strength for CFRP vitrimer composite following ASTM D3410 standard. \*Due to pretransitional softening on approaching the  $T_g$ .

| Environment  | Young's modulus (Gpa) |          | Mechanical strength |          |           |
|--------------|-----------------------|----------|---------------------|----------|-----------|
|              | Expected              | Measured | Expected            | Measured | Agreement |
| -70 to -40°C | 38                    | 38–39    | 360                 | 344      | Good      |
| +25°C        | 38                    | 35–72    | 360                 | 95–225   | Fair      |
| +60 to +90°C | 38                    | N/A      | 360                 | N/A      | Poor*     |

At high temperature, compression tests failed to produce reliable values. Measurements in the three point bending mode (Table S4) demonstrated that the flexural modulus of composite plates specimens decreases by about one order of magnitude between 25 and 60°C, thus confirming the effect of matrix softening.

### **Vitrimer-like properties**

Stress relaxation properties of the cured matrix (Figure S14) were measured and show that increasing temperature (from 180 to 200°C) leads to faster relaxation, but slackening above 200°C, probably due to formation of ether links by intermolecular dehydration.<sup>40</sup> However, it is noticeable that full relaxation is not achieved at any temperature within a measurable timescale and consequently this matrix will be referred as 'vitrimer like' by analogy with materials showing

the same structure and properties.<sup>45,46</sup> This can be explained by the nature of the network. The epoxy monomer used in this work has an average functionality of 3.6 epoxy function per molecule and CHDA a functionality of 2 acid functions per molecule. Following the reasoning of ref<sup>35</sup>, expected conversion at the gel point for the 1:1 stoichiometry is 62%. This is the case only if transesterification reactions are not considered. If transesterification reactions are considered, conversion at gel point shifts to 56%. Thus, transesterification reactions do not influence much the gelation of the system.

However, when comparing time to gel point determined at 130°C (Figure S3) with conversion obtained in IR measurement (Figure 3B), it appears that gelation happens at much lower conversion (20%) than expected. This demonstrates that side reactions are occurring: alcohol + epoxy reaction was mentioned above; the anionic ring opening polymerization of epoxies can be also considered for off-stoichiometric compositions.<sup>32,35</sup> This reaction is likely to take place here, due to incomplete melting of the trans-CHDA isomer. Both lead to ether bonds formation which are not exchangeable, making the network unable to reach full relaxation. The network is therefore considered as a vitrimer-like materials still able to bond or heal.

As a proper protocol is yet to be determined in order to measure relaxation of CFRP vitrimer and reshaping is rather limited by the fibers<sup>24</sup>, our focus went on showing interest of such CFRP vitrimer for sustainable applications: capacity of cracks healing, adhesion without the use of glue or bolts, and recovery of fibers at the end of the composite's life cycle. Crack healing and samples welding rely both on the system capacity to undergo transesterification upon heating (Figure 7). Firstly, we chose a damaged sample showing signs of delamination induced by the dry cutting mode. After flattening at 180°C for 30min, it can be seen that the fibers adhered to the matrix, reducing initial delamination which can be induced either during manufacturing or

processing or the CFRP composite plate (Figure 7). After flattening, six samples were taken to form lap-shear specimens according to procedure explained earlier. To measure the strength of the adhesion, lap-shear tests were performed, the samples were pulled 4 times to 1 kN pulling force ( $\approx 4$  MPa) without break, showing shear strength equivalent to classical epoxy glue. Upon 5th pulling event, one of the samples broke at the interface (Figure S18). Post mortem examination of the fracture surface showed evidence of cohesive fracture and that the effective contact was smaller than the overlap surface; meaning that the intrinsic debonding strength is between 4 and 6 MPa. This indicated that adhesion of the two CFRP pieces was achieved through effective welding of the matrix, permitted by the vitrimer bond exchanges mechanism.

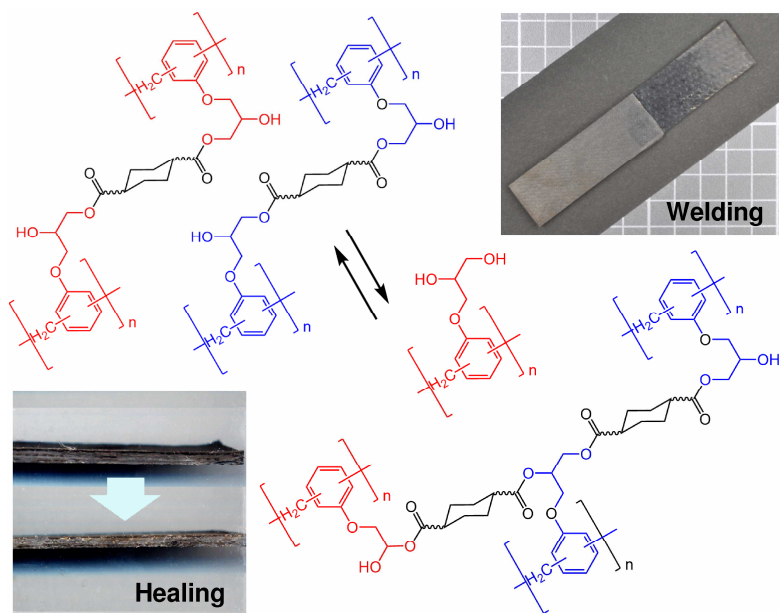


**Figure 7:** Cracks healing and adhesion through chemical exchange leading to bonding strength around 5 MPa.

Finally, as one of the main issues of thermoset CFRP is the end of life, with recycling leading to potential environmental wastes and degradation of the expensive carbon fibers, we took a small sample (2 cm × 1cm) to investigate the soft chemical depolymerization of the vitrimer matrix. The sample was plunged into an ethanol/acetone solution (50:50), and heated for 4h at 180°C in a pressurized reactor. After removal and cooling, the fiber sheets were separated with the help of a spatula and recovered. Figure 1 shows the full story from monomers to CFRP with vitrimer properties and eventually chemical depolymerization allowing fibers recovery. Despite small damage induced by the separation process, it is clear that the depolymerization allows to separate laminates in the size of the initial sample without the use of high temperature or harsh chemical usually used to remove classical thermoset epoxy resin.

Product of the depolymerization was analyzed with GPC (Figure S19) and compared to initial monomers, the trace overlay shows a larger proportion of higher oligomers in the depolymerization mixture, consistent with the occurrence of etherification side reactions above discussed.

## **Conclusions and outcomes**

The use of a heterogeneous reactive mixture (liquid epoxy and crystalline hardener) shows potential to produce long latency prepreg sheets and CFRP composites with vitrimer properties and demonstrated to be feasible on an industrial platform. When the hardener is chosen to be insoluble at ambient temperature, tackiness and viscosity are governed by the epoxy resin properties, allowing impregnation, layup and storage. Insured by the low reactivity of components and without need of cold storage, up to 25 days of latency are allowed by the chosen composition. If the mix remains below its homogenization temperature, the layup can also be

undone and remade in another configuration due to the high latency of the system. Simple combination of thermalized IR spectroscopy and optical microscopy was used to determine impregnation and homogenization temperatures which allowed to prepare and handle the prepreg vitrimer without risk of premature curing. The impregnation, made in an industrial environment, demonstrates an ease of transferring the vitrimer technology where it is still lacking applications: high performance CFRP composites.

As for the PPGEF/CHDA system, the current preliminary results on such CFRP composites demonstrates that vitrimer properties, such as crack healing, adhesion without bolts or glues (for weight reduction) or reactive depolymerization can ameliorate both life cycle and end of life of the materials. Nonetheless, outgassing and mechanical results (at high temperatures) also emphasize remaining margin of progress in the development of vitrimer resins for space applications. The broad glass transition and pretransitional softening of vitrimers when approaching  $T_g$  are currently limiting factors for their use in high performance CFRP. Formulation of high glass transition vitrimer, would need to carefully consider up to which temperature the system exhibits high strength. Increasing these properties means reducing chains mobility and getting closer to the degradation temperature of the polymers (either through unwanted secondary reaction or proper thermal degradation). This reduces the temperature windows to obtain healing or adhesion. Recent progress in high glass transition temperature vitrimer suggest this issue is solvable through careful design of the formulation. Hence, there is no doubt that heterogeneous systems with high latency can be used for prepregs FRP combining both requirement of thermoset resins and the dynamic properties of vitrimers.

**Supporting information.** Strategy to impart vitrimer properties in a latent epoxy formulation; IR band assignment; fiber content; activation energies; IR and rheology monitoring, optical microscopy of curable compositions; latency in presence of catalyst; stress relaxation and thermal degradation of cured compositions; preparation of large size preimpregnated sheets; composites' outgassing, three point bending, facies of fracture after bonding and analysis of the depolymerization products.

## **Acknowledgements**

ESPCI, CNRS, the Thales Group and the European Space Agency (ESA Contract 4000128430/19/NL/KML/afm) are thanked for financial support. Anton Paar France SAS is gratefully acknowledged for loan of the MCR702 rheometer. Paolo Edera is thanked for help in three-point bending measurements. Mickaël Pomès Hadda (CNRS), Maelys Lahoré (TAS) and Renaud Viala Artigues (Kalliste Composite) are thanked for technical support in resin, textile and composite handling.

## References

- (1) Mangalgi, P. D. Composite Materials for Aerospace Applications. *Bull. Mater. Sci.* **1999**, 22 (3), 657–664. <https://doi.org/10.1007/BF02749982>.
- (2) Diamanti, K.; Soutis, C. Structural Health Monitoring Techniques for Aircraft Composite Structures. *Prog. Aerosp. Sci.* **2010**, 46 (8), 342–352. <https://doi.org/10.1016/j.paerosci.2010.05.001>.
- (3) Jin, F. L.; Li, X.; Park, S. J. Synthesis and Application of Epoxy Resins: A Review. *J. Ind. Eng. Chem.* **2015**, 29, 1–11. <https://doi.org/10.1016/j.jiec.2015.03.026>.
- (4) Rebizant, V.; Venet, A. S.; Tournilhac, F.; Girard-Reydet, E.; Navarro, C.; Pascault, J. P.; Leibler, L. Chemistry and Mechanical Properties of Epoxy-Based Thermosets Reinforced by Reactive and Nonreactive SBMX Block Copolymers. *Macromolecules* **2004**, 37 (21), 8017–8027. <https://doi.org/10.1021/ma0490754>.
- (5) Vidil, T.; Tournilhac, F.; Musso, S.; Robisson, A.; Leibler, L. Control of Reactions and Network Structures of Epoxy Thermosets. *Prog. Polym. Sci.* **2016**, 62, 126–179. <https://doi.org/10.1016/j.progpolymsci.2016.06.003>.
- (6) Oliveux, G.; Dandy, L. O.; Leeke, G. A. Current Status of Recycling of Fibre Reinforced Polymers: Review of Technologies, Reuse and Resulting Properties. *Prog. Mater. Sci.* **2015**, 72, 61–99. <https://doi.org/10.1016/j.pmatsci.2015.01.004>.
- (7) Montarnal, D.; Capelot, M.; Tounilhac, F.; Leibler, L. Silica-Like Malleable Materials from Permanent Organic Network. *Science (80-. )*. **2011**, 334, 965–968.
- (8) Capelot, M.; Unterlass, M. M.; Tournilhac, F.; Leibler, L. Catalytic Control of the Vitrimer Glass Transition. *ACS Macro Lett.* **2012**, 1 (7), 789–792. <https://doi.org/10.1021/mz300239f>.

- (9) Altuna, F. I.; Hoppe, C. E.; Williams, R. J. J. Epoxy Vitrimers: The Effect of Transesterification Reactions on the Network Structure. *Polymers (Basel)*. **2018**, *10* (1), 43. <https://doi.org/10.3390/polym10010043>.
- (10) Ricarte, R. G.; Tournilhac, F.; Cloître, M.; Leibler, L. Linear Viscoelasticity and Flow of Self-Assembled Vitrimers: The Case of a Polyethylene/Dioxaborolane System. *Macromolecules* **2020**, *53* (5), 1852–1866. <https://doi.org/10.1021/acs.macromol.9b02415>.
- (11) Poutrel, Q. A.; Baghdadi, Y.; Souvignet, A.; Gresil, M. Graphene Functionalizations: Conserving Vitriemer Properties towards Nanoparticles Recovery Using Mild Dissolution. *Compos. Sci. Technol.* **2021**, *216* (July), 109072. <https://doi.org/10.1016/j.compscitech.2021.109072>.
- (12) Yu, K.; Shi, Q.; Dunn, M. L.; Wang, T.; Qi, H. J. Carbon Fiber Reinforced Thermoset Composite with Near 100% Recyclability. *Adv. Funct. Mater.* **2016**, *26* (33), 6098–6106. <https://doi.org/10.1002/adfm.201602056>.
- (13) Hamel, C. M.; Kuang, X.; Chen, K.; Qi, H. J. Reaction-Diffusion Model for Thermosetting Polymer Dissolution through Exchange Reactions Assisted by Small-Molecule Solvents. *Macromolecules* **2019**, *52* (10), 3636–3645. <https://doi.org/10.1021/acs.macromol.9b00540>.
- (14) Perego, A.; Lazarenko, D.; Cloitre, M.; Khabaz, F. Microscopic Dynamics and Viscoelasticity of Vitrimers. *Macromolecules* **2022**, *55* (17), 7605–7613. <https://doi.org/10.1021/acs.macromol.2c00588>.
- (15) Zhang, S.; Pan, L.; Xia, L.; Sun, Y.; Liu, X. Dynamic Polysulfide Shape Memory Networks Derived from Elemental Sulfur and Their Dual Thermo-/Photo-Induced Solid-State Plasticity. *React. Funct. Polym.* **2017**, *121*, 8–14.

<https://doi.org/https://doi.org/10.1016/j.reactfunctpolym.2017.10.005>.

- (16) Liu, Z.; Zhang, C.; Shi, Z.; Yin, J.; Tian, M. Tailoring Vinylogous Urethane Chemistry for the Cross-Linked Polybutadiene: Wide Freedom Design, Multiple Recycling Methods, Good Shape Memory Behavior. *Polymer (Guildf)*. **2018**, *148*, 202–210. <https://doi.org/https://doi.org/10.1016/j.polymer.2018.06.042>.
- (17) Li, A.; Fan, J.; Li, G. Recyclable Thermoset Shape Memory Polymers with High Stress and Energy Output via Facile UV-Curing. *J. Mater. Chem. A* **2018**, *6* (24), 11479–11487. <https://doi.org/10.1039/C8TA02644K>.
- (18) Lv, Y.; Lu, B.; Zhang, S.; Li, J.; Lu, G.; Sun, H.; Liang, S.; Liu, Z. Mechanical Enhancement of Amine-Functionalized TiO<sub>2</sub> Reinforced Polyimine Composites. *J. Appl. Polym. Sci.* **2018**, *135* (27), 46446. <https://doi.org/10.1002/app.46446>.
- (19) Azcune, I.; Odriozola, I. Aromatic Disulfide Crosslinks in Polymer Systems: Self-Healing, Reprocessability, Recyclability and More. *Eur. Polym. J.* **2016**, *84*, 147–160. <https://doi.org/10.1016/j.eurpolymj.2016.09.023>.
- (20) Huang, J.; Zhang, L.; Tang, Z.; Wu, S.; Guo, B. Reprocessable and Robust Crosslinked Elastomers via Interfacial C–N Transalkylation of Pyridinium. *Compos. Sci. Technol.* **2018**, *168* (July), 320–326. <https://doi.org/10.1016/j.compscitech.2018.10.017>.
- (21) Zheng, H.; Liu, Q.; Lei, X.; Chen, Y.; Zhang, B.; Zhang, Q. Performance-Modified Polyimine Vitrimers: Flexibility, Thermal Stability and Easy Reprocessing. *J. Mater. Sci.* **2018**. <https://doi.org/10.1007/s10853-018-2962-4>.
- (22) Demongeot, A.; Groote, R.; Goossens, H.; Hoeks, T.; Tournilhac, F.; Leibler, L. Cross-Linking of Poly(Butylene Terephthalate) by Reactive Extrusion Using Zn(II) Epoxy-Vitrimer Chemistry. *Macromolecules* **2017**, *50* (16), 6117–6127.

<https://doi.org/10.1021/acs.macromol.7b01141>.

- (23) Han, H.; Xu, X. Poly(Methyl Methacrylate)–Epoxy Vitrimer Composites. *J. Appl. Polym. Sci.* **2018**, *135* (22), 1–5. <https://doi.org/10.1002/app.46307>.
- (24) Chabert, E.; Vial, J.; Cauchois, J.-P.; Mihaluta, M.; Tournilhac, F. Multiple Welding of Long Fiber Epoxy Vitrimer Composites. *Soft Matter* **2016**, *12* (21), 4838–4845. <https://doi.org/10.1039/C6SM00257A>.
- (25) Yu, L.; Zhu, C.; Sun, X.; Salter, J.; Wu, H.; Jin, Y.; Zhang, W.; Long, R. Rapid Fabrication of Malleable Fiber Reinforced Composites with Vitrimer Powder. *ACS Appl. Polym. Mater.* **2019**, *1* (9), 2535–2542. <https://doi.org/10.1021/acsapm.9b00641>.
- (26) Memon, H.; Wei, Y.; Zhang, L.; Jiang, Q.; Liu, W. An Imine-Containing Epoxy Vitrimer with Versatile Recyclability and Its Application in Fully Recyclable Carbon Fiber Reinforced Composites. *Compos. Sci. Technol.* **2020**, *199*, 108314. <https://doi.org/10.1016/j.compscitech.2020.108314>.
- (27) Ruiz De Luzuriaga, A.; Martin, R.; Markaide, N.; Rekondo, A.; Cabañero, G.; Rodríguez, J.; Odriozola, I. Epoxy Resin with Exchangeable Disulfide Crosslinks to Obtain Reprocessable, Repairable and Recyclable Fiber-Reinforced Thermoset Composites. *Mater. Horizons* **2016**, *3* (3), 241–247. <https://doi.org/10.1039/c6mh00029k>.
- (28) Kissounko, D. A.; Taynton, P.; Kaffer, C. New Material: Vitrimers Promise to Impact Composites. *Reinf. Plast.* **2018**, *62* (3), 162–166. <https://doi.org/https://doi.org/10.1016/j.repl.2017.06.084>.
- (29) De Gennes, P. G.; J., P. *The Physics of Liquid Crystals*, 2nd Ed.; Clarendon Press, O., Ed.; 1993.
- (30) Fritsch, L.; Merlo, A. A. An Old Dog with New Tricks: Schiff Bases for Liquid Crystals

- Materials Based on Isoxazolines and Isoxazoles. *ChemistrySelect* **2016**, *1* (1), 23–30. <https://doi.org/10.1002/slct.201500044>.
- (31) Castellano, J. A.; Harrison, K., J. *Liquid Crystal Devices.*, in Sprokel.; Eds, J., 1975. <https://doi.org/10.1201/9781003210283-9>.
- (32) Tangthana-umrung, K.; Poutrel, Q. A.; Gresil, M. Epoxy Homopolymerization as a Tool to Tune the Thermo-Mechanical Properties and Fracture Toughness of Vitrimers. *Macromolecules* **2021**. <https://doi.org/10.1021/acs.macromol.1c00861>.
- (33) Chen, J. H.; An, X. P.; Li, Y. D.; Wang, M.; Zeng, J. B. Reprocessible Epoxy Networks with Tunable Physical Properties: Synthesis, Stress Relaxation and Recyclability. *Chinese J. Polym. Sci. (English Ed.* **2018**, *36* (5), 641–648. <https://doi.org/10.1007/s10118-018-2027-9>.
- (34) Demongeot, A.; Mougner, S.-J. J.; Okada, S.; Soulié-Ziakovic, C.; Tournilhac, F. Coordination and Catalysis of Zn<sup>2+</sup> in Epoxy-Based Vitrimers. *Polym. Chem.* **2016**, *7* (27), 4486–4493. <https://doi.org/10.1039/C6PY00752J>.
- (35) Poutrel, Q. A.; Blaker, J. J.; Soutis, C.; Tournilhac, F.; Gresil, M. Dicarboxylic Acid-Epoxy Vitrimers: Influence of the off-Stoichiometric Acid Content on Cure Reactions and Thermo-Mechanical Properties. *Polym. Chem.* **2020**, *11* (33), 5327–5338. <https://doi.org/10.1039/d0py00342e>.
- (36) Ooi, S. K.; Cook, W. D.; Simon, G. P.; Such, C. H. DSC Studies of the Curing Mechanisms and Kinetics of DGEBA Using Imidazole Curing Agents. *Polymer (Guildf)*. **2000**, *41* (10), 3639–3649. [https://doi.org/10.1016/S0032-3861\(99\)00600-X](https://doi.org/10.1016/S0032-3861(99)00600-X).
- (37) Woo, E. M.; Seferis, J. C. Cure Kinetics of Epoxy/Anhydride Thermosetting Matrix Systems. *J. Appl. Polym. Sci.* **1990**, *40* (7–8), 1237–1256.

<https://doi.org/10.1002/app.1990.070400713>.

- (38) Vidil, T.; Tournilhac, F. Supramolecular Control of Propagation in Cationic Polymerization of Room Temperature Curable Epoxy Compositions. *Macromolecules* **2013**, *46* (23), 9240–9248. <https://doi.org/10.1021/ma401720j>.
- (39) Vidil, T.; Tournilhac, F.; Leibler, L. Control of Cationic Epoxy Polymerization by Supramolecular Initiation. *Polym. Chem.* **2013**, *4* (5), 1323–1327. <https://doi.org/10.1039/c2py21140h>.
- (40) Chappuis, S.; Edera, P.; Cloitre, M.; Tournilhac, F. Enriching an Exchangeable Network with One of Its Components: The Key to High- TgEpoxy Vitrimers with Accelerated Relaxation. *Macromolecules* **2022**, *55* (16), 6982–6991. <https://doi.org/10.1021/acs.macromol.2c01005>.
- (41) Vidil, T.; Cloître, M.; Tournilhac, F. Control of Gelation and Network Properties of Cationically Copolymerized Mono- and Diglycidyl Ethers. *Macromolecules* **2018**, *51* (14), 5121–5137. <https://doi.org/10.1021/acs.macromol.8b00406>.
- (42) Stockmayer, W. H. Theory of Molecular Size Distribution and Gel Formation in Branched-Chain Polymers. *J. Chem. Phys.* **1943**, *11* (2), 45–55. <https://doi.org/10.1063/1.1723803>.
- (43) Bakkali-Hassani, C.; Edera, P.; Langenbach, J.; Poutrel, Q. A.; Norvez, S.; Gresil, M.; Tournilhac, F. Epoxy Vitrimer Materials by Lipase-Catalyzed Network Formation and Exchange Reactions. *ACS Macro Lett.* **2023**, 338–343. <https://doi.org/10.1021/acsmacrolett.2c00715>.
- (44) Jourdain, A.; Obadia, M. M.; Duchet-Rumeau, J.; Bernard, J.; Serghei, A.; Tournilhac, F.; Pascault, J. P.; Drockenmuller, E. Comparison of Poly(Ethylene Glycol)-Based Networks

Obtained by Cationic Ring Opening Polymerization of Neutral and 1,2,3-Triazolium Diepoxy Monomers. *Polym. Chem.* **2020**, *11* (11), 1894–1905. <https://doi.org/10.1039/c9py01923e>.

- (45) Imbernon, L.; Norvez, S.; Leibler, L. Stress Relaxation and Self-Adhesion of Rubbers with Exchangeable Links. *Macromolecules* **2016**, *49* (6), 2172–2178. <https://doi.org/10.1021/acs.macromol.5b02751>.
- (46) Kaiser, S.; Wurzer, S.; Pilz, G.; Kern, W.; Schlögl, S. Stress Relaxation and Thermally Adaptable Properties in Vitrimer-like Elastomers from HXNBR Rubber with Covalent Bonds. *Soft Matter* **2019**, *15* (30), 6062–6072. <https://doi.org/10.1039/c9sm00856j>.

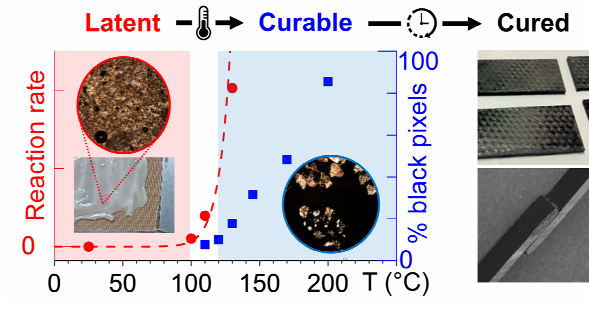


Table of Contents (TOC) graphic